Excited-state absorption of Eu^{2+}-doped materials

J. K. Lawson and Stephen A. Payne

University of California, Lawrence Livermore National Laboratory, P.O. Box 5508, L-490, Livermore, California 94550

(Received 20 October 1992)

We have investigated the excited-state absorption spectra of four Eu^{2+}-doped materials: CaF_2, SrF_2, $SrCl_2$, and $LiCaAlF_6$. The excited-state absorption in the emission region of each material is similar in nature to that previously observed for CaF_2, and is suggested to arise from a $5d \rightarrow$ (conduction band) transition. An electrostatic model for the onset of this type of transition is successful in predicting trends among different hosts.

I. INTRODUCTION

The bright blue luminescence characteristic of Eu^{2+}-doped materials has enticed many researchers to search for blue laser systems based on this divalent ion. However, no one has reported gain in any of the numerous of hosts in which Eu^{2+} can be incorporated. An explanation for the lack of gain came from Owen, Dorian, and Kobayasi[1] who found strong excited-state absorption (ESA) in the emission region of CaF_2:Eu^{2+}. Recent studies[2–4] have found similar ESA features in alkali halide hosts, although the emission region was not actually studied in these cases. Unfortunately, the presence of Eu^{2+} clusters and varied charge compensators serve to confuse the interpretation if these ESA spectra. Here, we systematically investigate the nature of the ESA observed in several different hosts in order to better understand whether the mechanism which inhibits the gain in
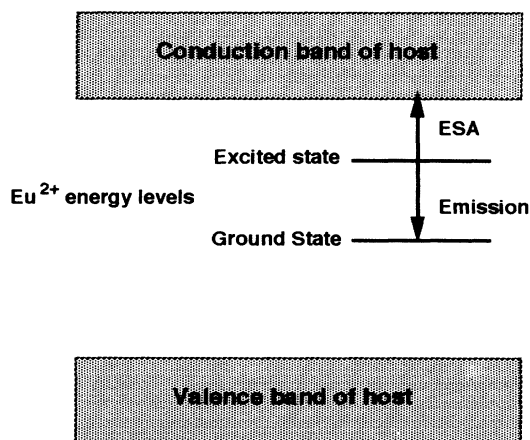

FIG. 1. The energy levels of Eu^{2+} reside in the band gap of the host. Excited-state absorption (ESA) defeats gain when the wavelength of a transition between the excited state and the conduction band overlaps that of the emission.

CaF_2:Eu^{2+} affects all Eu^{2+}-based systems.

Based on the oscillator strength, width, and spectral position of the ESA band, Owen, Dorain, and Kobayasi[1] tentatively suggested that the ESA transition was due to the transfer of an electron from the $5d$ orbital of the impurity ion to the conduction band (CB) of the host (Fig. 1), although he also discussed the possibility of it arising from a $5d$-$5d$-type transition. This $5d \rightarrow$ CB assignment relied heavily on the theory developed by Pedrini, McClure, and Anderson,[5] which estimated the position of the divalent impurity's energy levels in the band gap of the host. Although transitions in which an electron transfers from an impurity ion to the CB of the host have commonly been observed in semiconductors, it remains an unusual feature to be observed for impurity ions doped into insulators. In fact, it represents one of the few instances of localized $\rightarrow$ delocalized transitions seen in insulators.

During the course of our previous work on Sm^{2+},[6] we observed an ESA band similar in nature to that seen for Eu^{2+}. Although the ESA does not overlap the emission region in CaF_2:Sm^{2+} and does not prevent gain, basic similarities of Eu^{2+} and Sm^{2+} (such as the ground-state electronic configurations being $4f^7$ and $4f^6$, respectively) suggest that the insights gained for Sm^{2+} may be directly applicable to Eu^{2+}. We have shown that the onset of the $5d \rightarrow$ CB transition for Sm^{2+} in various fluorite hosts can be predicted using an electrostatic model originally developed to model the photoionization thresholds of divalent ions in fluorite hosts.[7] Here, we attempt to expand on previous calculations in order to model the onset of the ESA band for Eu^{2+} in various hosts.

II. BACKGROUND

A. Electronic configuration

The bulk of information about rare-earth ions concerns the trivalent ions, since the $3+$ oxidation state is the energetically preferred valency. However, Eu^{2+}, Sm^{2+}, and Yb^{2+} are known to have stable divalent states. A survey paper recently written by Rubio[8] summarizes much of

the spectroscopic information available for these divalent ions.

The free ion energy levels for Eu^{2+} were obtained by Sugar and Spector[9] and are shown in Fig. 2. The ground-state electronic configuration of Eu^{2+} is that of a half-filled $4f$ shell, i.e, $4f^7$. This results in a $^8S_{7/2}$ level for the ground state. The next $4f^7$ manifold (^6P_J) lies approximately 28 000 cm^{-1} higher. The lowest-lying $4f^65d$ levels begin near 34 000 cm^{-1} and are labeled ^8H_J for the free ion. The $4f^65d$ levels experience much more crystal-field splitting than the $4f^7$ levels due to the increased spatial extent of the $5d$ orbital (thousands of cm^{-1} vs hundreds of cm^{-1}), and often are the metastable state, or the lowest excited state, when the free ion is incorporated in a crystalline host.

Much of the information available for Eu^{2+} is for the ion in alkaline-earth fluorides or alkali halides.[10-29] The initial interpretation of the data for crystals confirmed the presence of a low-lying $4f^55d$ band, which is found to be much more sensitive to the crystal-field effects than levels arising from the highly shielded $4f$ orbitals. Al-
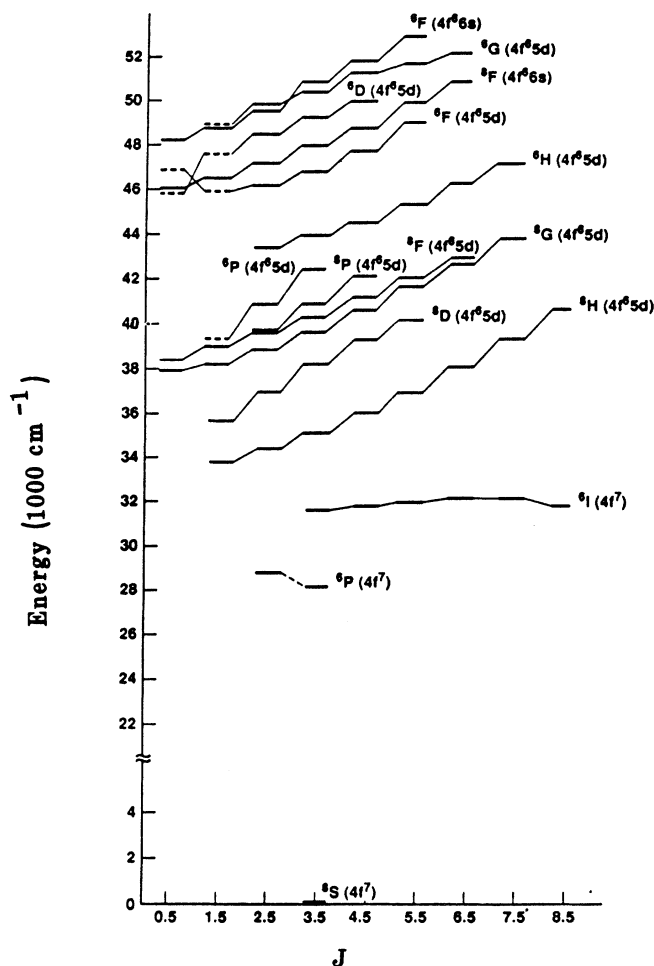
though the broad bands apparent in the absorption and emission spectra of alkali and alkaline-earth halide crystals were quickly associated with the $5d$ orbital (see for example Ref. 10), the structure of the bands and the complex coupling of the $4f^6$ and $5d$ orbitals at first was not well understood. Yanase and Kasuya[19] refined the suggestion made by Freiser, Methfessel, and Holtzberg[17] that the interactions between the $5d$ and $4f$ electrons are small and can be neglected to first order, by showing that a fortuitous cancellation of the multipole-multipole Coulomb interactions and the anisotropic exchange interactions occurs. They also noted that conventional LS-coupling schemes could not be usefully applied to a system where the cubic crystal-field shifts are as large or larger than the shifts due to LS coupling, since the crystal-field splitting of the $5d$ states is usually larger than 1 eV in cubic hosts. Thus, the notation for the $4f^65d$ bands in crystalline hosts that we use is not the standard LS notation, but is based on the description of the $4f^65d$ state developed by Yanase and Kasuya.

In Yanase and Kasuya's description of the $4f^65d$ state, the effect of the crystal field on the $5d$ electron is first considered and noted to split the $5d$ orbitals into two components, t_{2g} and e_g. The isotropic part of the exchange interaction between the $5d$ and $4f$ electrons results in an exchange splitting into states with total spins of $S = \frac{7}{2}$ and $\frac{5}{2}$. Thus, for the absorption spectra of Eu^{2+} in the fluorite structure hosts studied (as shown in Fig. 3), the lowest energy band arises from the state described by the notation $|4f^6(^7F_J) e_g, S = \frac{7}{2}\rangle$. Note that the lowest energy configuration corresponds to the situation where the $^7F_J(4f^6)$ state couples to the $5d$ e_g orbital such that all the spins are parallel.

The relative strength of the various electron interactions was supported by the electron spin resonance measurements of the metastable $4f^65d$ level of Eu^{2+} in CaF_2, SrF_2, and BaF_2 by Chase.[20] He interpreted his results as resulting from a large crystal-field splitting of the $5d$ electron and a considerably smaller coupling of this electron to the $4f^6$ configuration. In addition, he found the exchange coupling on the same order as the spin-orbit coupling for the $4f^65d$ configuration. Weakleim, Anderson, and Sabisky[21] also substantiated this type of coupling scheme by calculating the relative magnitude of the Coulomb and exchange interactions in the crystal environment. They showed that existing data was consistent with the coupling scheme outlined above.

B. Existing ESA measurements

Previous ESA measurements of Eu^{2+} exist, which begin to explain the reasons behind the lack of gain for Eu^{2+}-doped materials. Table I summarizes much of the relevant work reported to date. Owen, Dorain, and Kobayasi[1] suggested that the ESA band seen in $CaF_2:Eu^{2+}$ might be due to a $5d \rightarrow$ conduction band (CB) transition. Since then, Merkle, and co-workers[2,4] have studied the Eu^{2+}-doped salts and have seen a similar ESA band in KBr, KCl, NaCl, and NaF. Data recorded by Nagli and Karklinya[3] for $KCl:Eu^{2+}$ conflict somewhat

FIG. 2. The free-ion energy levels of Eu^{2+} [after Sugar and Spector (Ref. 9)].

from Merkle's results but again document the presence of a broad ESA band.

Several aspects of these data are remarkable. The large cross section, broad width, and the large shifts in position of the transition are very unusual for transitions involving rare-earth ions. The cross section are as large or larger than those for the allowed $4f$-$5d$ transitions (which are typically on the order of 10^{-18} cm^2). Both the full widths at half maximum (FWHM) and the host-dependent energy shifts in the position of the peak are on the order of an electron volt. These values are not typical for the localized transitions involving rare-earth ions. (Note that the broadest $4f \rightarrow 5d$ absorption bands are only about 0.5 eV wide.) However, the strength and width of the ESA bands are consistent with a transition involving the transfer of an electron. For this type of transition, large dipole moments would by typical and widths would be on the order of the conduction or valence bandwidths.
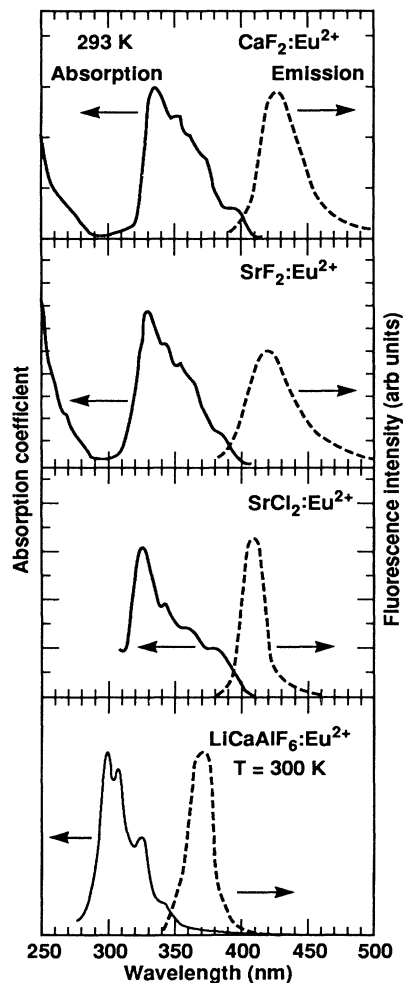
TABLE I. Summary of ESA data reported to date for Eu^{2+} in various hosts.

Host	ESA band properties			Peak cross section (10^{-18} cm^2)
	Onset	Peak	FWHM	
		(energies in eV)		
CaF_2 [a]	1.7	2.4	0.8	28
$NaCl$ [b]	< 3.1	4.2		(5–12)
KCl [c]		4.2	0.8	0.7
KCl [b]	< 3.1	4.0	1.1	(7–13)
KBr [b]		4.1	1.0	(10–19)
NaF [d]	1.9	2.6	1.0	0.6

[a]Reference 1.
[b]Reference 2. Values in brackets reflect uncertainty in the quantum efficiency.
[c]Reference 3.
[d]Reference 4.

Figure 4 describes schematically the difference in the two types of electron-transfer transitions that may exist. The analogy with transitions typically observed in semiconductors is apparent here. Charge-transfer transitions involve an electron from the valence band of the host being transferred to the impurity ion. This process corresponds to acceptor transitions and sometimes results in the subsequent formation of an exciton in semiconductors. The other possibility involves the transfer of an electron from the impurity to the host. This is the type of transition Owen, Dorain, and Kobayasi, tentatively proposed to explain the origin of the ESA band observed in CaF_2:Eu^{2+}. Although these two types of transitions are similar, they behave in opposite ways with respect to

FIG. 3. Absorption and emission spectra of the four materials investigated in this study [spectra of CaF_2, SrF_2, and $SrCl_2$ after Kobayasi, Mroszkowski, and Owen (Ref. 24); $LiCaAlF_6$ data was from our measurements].
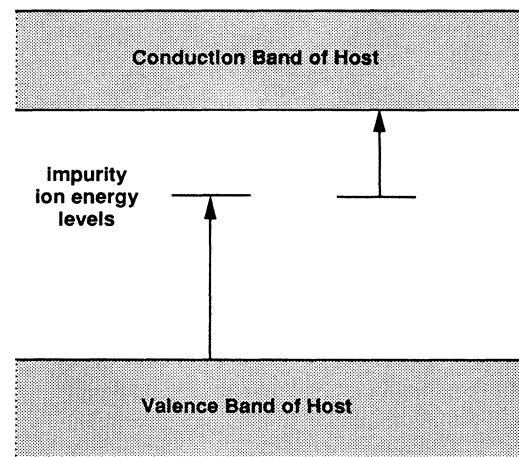

FIG. 4. Two possible transitions can occur involving the exchange of an electron between an impurity and the host medium. The electron can be transferred from the valence band of the host to the impurity, possibly forming an exciton (i.e., charge-transfer transition) or the electron can be transferred from an impurity ion, whose energy level reside in the band gap of the host, to the CB (i.e., as occurs in the $5d \rightarrow$ CB transition).

changes in the host or impurity. For example, if the halogen in the host is changed from fluorine to chlorine, the increased polarizability and enlarged lattice constant tend to increase the energy separation of the impurity energy levels from the conduction band of the host, while decreasing the gap from the valence band. A charge-transfer transition would therefore decrease in energy, while a impurity → host transition would increase in energy in passing from a fluoride to a chloride host medium.

C. Photoconductivity thresholds

Since the depth of the ground state of the ion in the band gap of the host plays a central role in determining the position of the ESA band, we have included published data (Table II) available on the photoconductivity threshold of the ions in the various hosts,[27−29] including both the theoretical and observed values. The close association of the ESA and photoconductivity data lies in the dependence of both processes on the transfer of an electron from the impurity to the CB of the host. In photoconductivity measurements, the depth of the ground state from the CB is directly measured as the amount of optical energy required to ionize the impurity and produce a source of measurable current in the sample. Since we know the energy difference of the ground $4f^7$ and metastable $4f^65d$ states of the impurity ion from absorption and emission data, the photoconductivity threshold allows us to estimate the onset of the $5d \rightarrow$ CB transition. Unfortunately, photoconductivity measurements are sensitive to the presence of impurities and defects in the sample. The threshold measured is that of the first species in the sample to ionize. If that species is not the one intended for study, the results of the photoconductivity measurements are confusing and open to misinterpretation.

Experimental photoconductivity data exist for many of the divalent ions in various fluorite hosts. Early measurements by Pedrini, Rogemond, and McClure of the photoconductivity threshold of Eu^{2+} in fluorite were significantly lower than predicted. However, recent studies by Fuller and McClure[29] of selective photoionization in the codoped SrF_2:Eu,Sm system showed that the photoionization of Eu^{2+} in SrF_2 actually had a much higher threshold than originally measured. They suggested that the lower value reported for the earlier data was associated with a fluorine compensated Eu^{2+} ion. New measurements have not been reported on CaF_2:Eu^{2+} although a similar situation may also exist here. Data for the alkali halides[28] recorded by de Cárcer, Cussó, and Jaque provide values of the photoionization threshold very similar to the alkaline-earth halides, although calculations using similar models for the two crystal structures produces very different magnitudes for the thresholds of the alkali halides. The actual electrostatic model used in these calculations and the possible source of the large discrepancy in the calculated and observed thresholds will be discussed in detail below.

D. Exciton luminescence

An interesting situation occurs in BaF_2:Eu^{2+} and CdF_2:Eu^{2+} that further illustrates the unique role the CB plays in the transitions of Eu^{2+} in crystalline hosts. Photoconductivity measurements of CdF_2:Eu^{2+} by Godlewski et al.[30] and of BaF_2:Eu^{2+} by Moine, Pedrini, and Courtois[31] showed that the $4f^65d$ levels of Eu^{2+} actually reside in the CB of these crystals. Furthermore, the emission from BaF_2:Eu^{2+} suffers an anomalous red shift. In this system, photoionization of the Eu^{2+} ion results in an electron being transferred from the impurity to the CB of the host. There it is quickly trapped into a large orbit by the attractive potential of the Eu^{3+} ion to form an exciton. The emission occurs when the exciton collapses back to the Eu^{2+} ion.

III. PUMP-PROBE EXPERIMENT

We recorded the pump-probe spectrum for Eu^{2+} in CaF_2, SrF_2, $SrCl_2$, and $LiCaAlF_6$ (LiCAF) over a broad spectral range (from approximately 250 to 800 nm). CaF_2 SrF_2, and $SrCl_2$ all possess the fluorite crystal structure and the effect of the impurity ion on the characteristic distances of the lattice is well understood. The rare-earth ion occupies the metal site and is surrounded by the halides in eightfold coordination. $LiCaAlF_6$, in contrast, has the colquiriite ($ABCF_6$) structure.[32] The divalent rare earth will occupy the Ca^{2+} site and see a sixfold coordination of fluorines. With this selection of hosts, we can examine both the result of systematic changes in the eightfold-coordinated anion environment within a single structure (i.e., fluorite) and also the result from the change of both the coordination (eightfold→sixfold) and structure (fluorite→colquiriite).

In order to cover a broad spectral range, we used two

TABLE II. Summary of photoconductivity data reported to date for Eu^{2+} in various hosts.

Host	Photoionization threshold (eV)	
	Obs.	Calc.
CaF_2	$(3.8)^{a,b}$	5.25^b
SrF_2	4.7^c	4.45^b
NaCl	4.5^d	$6.6-8.0^e$
KCl	4.4^d	$6.7-8.5^e$
KBr	3.7^d	$7.0-9.0^e$
NaF		$4.9-6.1^f$

[a]This result may be due to an anomalous site; subsequent study is needed.
[b]Reference 27.
[c]Reference 29.
[d]Reference 28.
[e]Reference 2.
[f]Reference 4.

separate pump-probe arrangements. The arrangement shown in Fig. 5 used a flashlamp probe to cover a broad spectral region, although the flashlamp lacked sufficient spectral intensity in the emission region to overcome the background generated by fluorescence from the sample. Fortunately, the fluorescence only effects data collected inside the emission region, leaving a large spectral region of use to the experimenter. The light transmitted by the sample was collected into a spectrometer, whose output was recorded by an EG&G Princeton Applied Research optical multichannel analyzer (OMA). The spectrum was obtained in the presence and absence of the pump by the OMA and later transferred to an IBM computer, which calculated the pump-probe spectrum.

In order to study the emission region, we used a dye laser probe arrangement (Fig. 6). Different spectral regions could be reached either by choosing the appropriate blue dye (Coumarin or Stilbene), or by frequency converting one of the efficient Rhodamine dyes to produce tunable blue light. The frequency conversion schemes used potassium dihydrogen phosphate or β-barium borate to double the dye output or to mix the dye output with one of the Nd:YAG harmonics. The methods employed to produce the laser probe resulted in a variety of output powers ranging from millijoules for the Coumarin dyes to microjoules for the least efficient mixing schemes. Probe intensity fluctuations and the probe transmission of the sample were monitored by Molectron J-3 pyroelectric detectors unless the lack of sensitivity required the use of voltage biased diodes. The diodes were operated in a region where the linearity of the response was verified. The outputs of the detectors were collected by Standard Research Systems (SRS) boxcar averagers. Data were retrieved from the boxcars using a SRS computer interface connected to an IBM computer via a National Instrumnets general purpose interface bus. The computer interface also allowed the computer to control scanning of the dye laser and the opening and closing of various shutters. Data were collected for the pumped and unpumped state and recorded as

$$A_d = -ln(I_p/I_u) \,, \tag{1}$$

where I_p and I_u are the intensities of the transmitted probe with and without the pump overlapped spatially
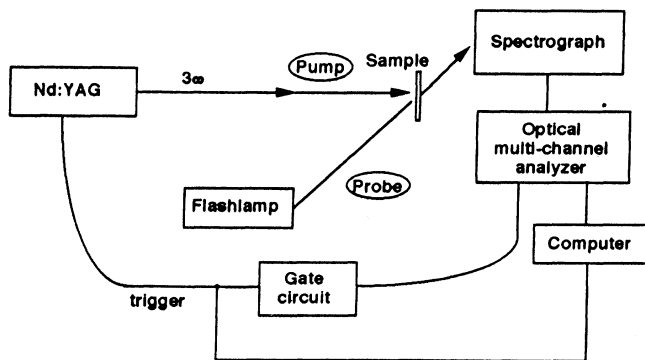

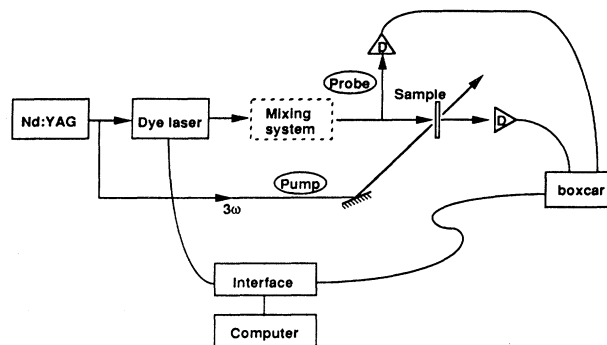FIG. 5. Flashlamp probe experimental arrangement.

FIG. 6. Laser probe experimental arrangement.

and temporally.

The information generated by both arrangements was merged into a single representation by scaling the various segments from the different dyes or from the flashlamp, taking care to match the magnitude and slope of the spectrum in the regions of overlap. When no overlap existed between two adjoining regions, we attempted to extrapolate through the missing region in a reasonable fashion.

IV. PUMP-PROBE SPECTRUM

Our results are shown in Fig. 7. Comparison with the absorption data (Fig. 3) demonstrates that the ground-state bleaching feature at 350 nm reproduces the absorption band faithfully. Slight evidence of a negative feature in the emission region (noted by the asterisk at 420 nm) suggests that the magnitude of the emission cross section is significantly smaller that of the absorption cross section. However, in each of the four hosts, a prominent ESA band overlaps the emission region.

The onset of this band differs strongly from host to host. The ESA spectrum that we recorded for CaF$_2$:Eu^{2+} agrees closely with the spectrum originally taken by Owen, Dorain, and Kobayasi.[1] The onset of the ESA band occurs at approximately 1.7 eV. The peak ESA cross section appears to be approximately 3.5 times the magnitude of the ground-state bleaching feature at 350 nm. The peak cross section for the ground-state absorption feature was measured by Arkhangelskaya, Kiselyeva, and Shraiber[15] to be 7.3×10^{-18} cm^2. This implies that the peak cross section of the ESA band is approximately 2.6×10^{-17} cm^2, in very close agreement with the value reported by Owen, Dorain, and Kobayasi[1] of 2.8×10^{-17} cm^2.

In SrF$_2$:Eu^{2+}, the onset of the ESA band is shifted over a hundred nanometers to the red, beyond the range which the OMA spectrometer was configured to detect. It appears that the ESA band begins around 850 nm, or 1.5 eV. The peak cross section of the ESA band is approximately 1.5 times the magnitude of the ground-state bleaching feature. The width of the band has also increased from that seen in CaF$_2$. This may be due to an increase in the width of the CB in SrF$_2$ vs CaF$_2$. In

$SrCl_2$:Eu^{2+}, the onset of the ESA band is shifted to much higher energies than either of the other two fluoride hosts, but still overlaps with the emission region. We estimate the onset of the ESA band to occur at 2.1 eV. The peak ESA cross section in this host is about 3 times the magnitude of the ground-state belaching feature. The width of the ESA band in this case appears comparable to that in CaF_2. Assuming that the ground-state absorption cross section in both of these hosts is comparable to that measured in CaF_2, we estimate the peak ESA cross section in SrF_2 and $SrCl_2$ to be 1×10^{-17} and 2×10^{-17} cm^2, respectively.

The crystal-field strength of $LiCaAlF_6$ is much less than the fluorite hosts, shifting the absorption and emission deeper into the untraviolet. The onset of the ESA band occurs at the highest energy among the hosts studied; it is near 2.2 eV. The peak ESA cross section is only 40% of the magnitude of the ground-state bleaching feature. Based on an inductively coupled plasma-mass spectrometry measurement of the europium concentration and measured optical density, we determined the
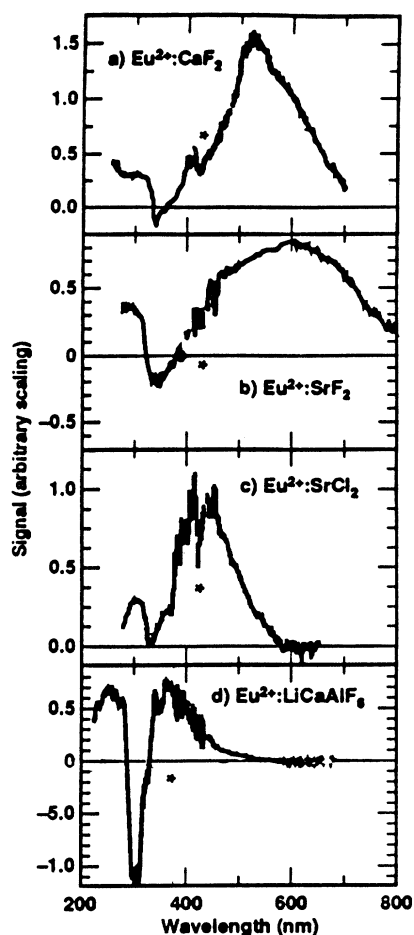

FIG. 7. Results of the pump-probe experiment show that the onset of the prominent ESA band varies widely with different hosts. The asterisks denote the peak positions of the emission bands.

value of the ground-state absorption cross section at 299 nm to be 4.3×10^{-18} cm^2. This implies that the peak ESA cross section is approximately 1.7×10^{-18} cm^2. Interestingly, the magnitude of the ESA band is much smaller in $LiCaAlF_6$ than in the fluorite hosts. This suggests a basic difference in the nature of the hosts strongly affects the strength of the ESA transition. The Eu^{2+} ion substitutes for the Ca^{2+} ion in $LiCaAlF_6$ and is surrounded by fluorine ions. In contrast to the fluorite hosts, the nearby metal ions are not alkaline-earth metals, but the highly ionic Li^+ and Al^{3+} ions. The increased ionic character of these ions possibly leads to a reduced level of overlap with the $Eu^{2+} 5d$ orbital. The overall effect of these ions on the structure of the conduction band, the $Eu^{2+} 5d$ orbitals and, ultimately, the $5d \rightarrow CB$ transition, is not readily obvious.

V. ANALYSIS

We used the electrostatic model developed previously by Pedrini, McClure, and Anderson[5] to predict photoionization thresholds for divalent rare-earth ions in fluorite hosts in order to better understand the existing ESA data and to explain our results. In essence, the electrostatic model places the ground state of the rare-earth ion in the band gap of the host (E_{pi}) by modifying the free-ion ionization potential (I_p) to account for the stabilization experienced by the ground state of the impurity ion in the host medium. This stabilization consists of the Madelung potential present at the impurity site (E_m), a correction to this potential to compensate for the polarizability of the anions (E_p), and a correction term to account for the changes in lattice distances that results from the substitution of the impurity for a host ion (ΔE):

$$E_{pi} = I_p - (E_m + E_p) + \Delta E \ . \tag{2}$$

We can gauge the distance of the $4f^6 5d$ excited state from the CB by subtracting the energy of the metastable $5d$ level (E_{ex}) from E_{pi}, the value calculated with the electrostatic model:

$$E_{esa} = E_{pi} - E_{ex} \ . \tag{3}$$

It is difficult to extend the electrostatic model to situations other than that for which it was originally intended, i.e., divalent ions in fluorite hosts. When modeling the stabilization that a divalent ion encounters when substituted into the metal site in a fluorite host, no charge compensation is involved and the extend of lattice relaxation due to the incorporation of the impurity ion was known from previous work. Thus, the description of the local environment of the rare-earth ion could be modeled accurately. The issues are much more complex in other cases, where for example, a divalent ion replaces a monovalent ion in an alkali halide with a rocksalt structure.

In order to use the electrostatic model for Eu^{2+}-doped alkali halides, Merkel assumed a simple charge compensation mechanism of a vacancy on a nearest neighbor cation site. A major difficulty arises, however, in approximating the lattice relaxation around the impurity ion. Merkle established limits for the possible values by calculating the onset of the ESA with no change in lattice

TABLE III. Analysis of observed Eu^{2+} ESA band in various hosts (all energies in eV).

Host	Measured ESA band onset	E_{esa} calc. $(E_{pi}-E_{ex})$	E_{pi} obs.	E_{pi} calc.	E_{ex}
CaF$_2$	1.7[a]	2.3		5.3[b]	3.0
SrF$_2$	1.5[c]	1.6	4.7[d]		3.1
SrCl$_2$	2.1[c]	3.2		6.2[b]	3.0
LiCaAlF$_6$	2.2[c]				3.4
NaCl	<3.1[e]	1.6	4.5[f]		2.9
KCl	<3.1[e]	1.5	4.4[f]		2.9
KBr		0.7	3.7[f]		3.0

[a]Reference 1.
[b]Reference 26.
[c]This work.
[d]Reference 28.
[e]Reference 3.
[f]Reference 27.

spacing, and again assuming that the equilibrium distances relax to those characteristic of the stoichiometric rare-earth dihalide (see Table II). This model does not correctly predict the onset of the ESA band, but does predict trends similar to those seen in the data. The large magnitude of the discrepancy originally led Merkle to consider charge transfer as the ESA mechanism, but the decrease in onset energy in going from bromide to chloride makes the assignment seem improbable.

In light of the difficulty in using the electrostatic model to estimate the depth of the ground state from the CB, the measured photoionization thresholds for Eu^{2+} in the alkali halides[28] may instead be used to predict the onset of the ESA band for Eu^{2+} in these materials. In fact, these data suggest that values calculated based on the electrostatic model overestimate the photoionization threshold by several electron volts.

The results of our calculations are given in Table III. The trends in the observed onset energies agree with the trends in the calculated measurements. Also included in the table are our estimates for the onset of the ESA band in the alkali halides based mainly on the measured photoconductivity thresholds (although the calculated E_{pi} values were used for CaF$_2$ and SrCl$_2$).

VI. DISCUSSION AND CONCLUSION

We have measured the pump-probe spectrum of Eu^{2+} in four hosts: CaF$_2$, SrF$_2$, SrCl$_2$, and LiCaAlF$_6$. In each case, a strong, broad ESA band overlaps the emission region, preventing gain. The ESA band seen in CaF$_2$ is consistent with the one reported by Owen, Dorain, and Kobayasi.[1] The strength, width, spectral position, and shape of the ESA band in each host suggest that the same type of transition is occurring in each case. The most likely source of the ESA band was suggested by Owen, Dorain, and Kobayasi as the transfer of an electron from the Eu^{2+} 5d orbital to the CB of the host.

The shift in the onset of the ESA band differs widely from host to host, although the trends are consistent with

our ability to judge the depth of the 5d levels from the conduction band using the electrostatic model developed by Pedrini, McClure, and Anderson.[5] In fact, the calculated onset of the ESA band for SrF$_2$:Eu^{2+} agrees closely with the measured onset. The agreement based on calculated photoionization thresholds for the other fluorites does not agree as closely, in general overestimating the value of the onset, although closely reflecting the trends. Without values for the onset of the ESA band in the alkali halides, it is difficult to do more than estimate the behavior of the ESA band. Nevertheless, the electrostatic model results in reasonable values for the ESA band in the alkali halides.

Our ability to model this transition is limited by the sparseness of existing knowledge about the interactions between the impurity and the CB of the host. This is one of the few cases of localized → delocalized transitions observed in insulators. We have found that the concepts developed for modeling the measured photoionization thresholds were critical in understanding the trends in the data. The 5d→CB ESA band may be, in fact, pervasive among the states of the divalent rare-earth ions where the 5d orbital plays a prominent role.

The photoionization problems experienced by Ce^{3+} lasers probably have their origin in the ESA transition described here. Although YLF:Ce and LaF$_3$:Ce have been shown to lase,[33,34] YLF:Ce in particular is plagued by problems due to photoionization. The pump-induced loss in this system was studied by Lim and Hamilton[35] who determined that the loss mechanism involved a transition from the 5d level of Ce^{3+} to the CB. Other attempts at finding a laser based on Ce^{3+} included studies of YAG and CaF$_2$.[1,36−39] These studies have also noted a strong ESA band identified with a 5d→ CB transition. In fact, Owen, Dorain, and Kobayasi[1] studied the ESA of YAG:Ce^{3+} as well as CaF$_2$:Eu^{2+} and found strong similarities between the two ESA transitions. They concluded with a general statement which emphasized the importance of the CB of the host in determining whether excited-state absorption would prevent laser action.

If the positive characteristics of the 5d→4f transition are to be fully exploited, we must explore the behavior of the 5d→CB transition in detail. The results presented here add a major piece to the existing puzzle. The onset of the ESA band can be shifted by a suitable choice of host. The reduced oscillator strength of the ESA band in presence of the sixfold coordination and crystal field experienced by Eu^{2+} in the colquiriite structure demonstrates the sensitivity of the ESA band to the choice of the host medium. Whether the reduction is due to the change in symmetry, difference in overlap of the ion and anion orbitals, or some other effect is not clear from our data. However, the width and strength of the band makes it difficult to shift the onset past the emission region for Eu^{2+}. Thus, it appears unlikely that any host exists in which Eu^{2+} will demonstrate gain.

[1]J. F. Owen, P. B. Dorain, and T. Kobayasi, J. Appl. Phys. **52**, 1216 (1981).

[2]L. D. Merkle and P. K. Bandyopadhyay, Phys. Rev. B **39**, 6939 (1989).

[3]L. E. Nagli and M. N. Karklinya, Opt. Spektresk. **67**, 1415 (1989) [Opt. Spectrosc. (USSR) **67**, 832 (1989)].

[4]L. D. Merkle, Phys. Rev. B **42**, 3783 (1990).

[5]C. Pedrini, D. S. McClure, and C. H. Anderson, J. Chem. Phys. **70**, 4979 (1979).

[6]J. K. Lawson and S. A. Payne, J. Opt. Soc. Am. **8**, 1404 (1991).

[7]J. K. Lawson, H. W. H. Lee, and S. A. Payne, *OSA Proceedings on Advanced Solid-State Lasers 10*, edited by G. Dubé and L. Chase (Optical Society of America, Washington, D.C., 1991), p. 386.

[8]J. Rubio O., J. Phys. Chem. Solids **52**, 101 (1991).

[9]J. Sugar and N. Spector, J. Opt. Soc Am. **64**, 1484 (1974).

[10]D. S. Butement, Trans. Faraday Soc. **44**, 617 (1948).

[11]P. P. Feofilov, Opt. Spektrosk. **1**, 992 (1956).

[12]A. A. Kaplyanskii and P. P. Feofilov, Opt. Spektrosk. **13**, 235 (1962) [Opt. Spectrosc. (USSR) **13**, 129 (1962)].

[13]D. S. McClure and Z. Kiss, J. Chem. Phys. **39**, 3251 (1963).

[14]R. Reisfeld and A. Glasner, J. Opt. Soc. Am. **54**, 331 (1964).

[15]V. A. Arkhangelskaya, M. N. Kiselyeva, and V. M. Shraiber, Opt. Spektrosk **23**, 509 (1967) [Opt. Spectrosc. (USSR) **23**, 275 (1967)].

[16]E. Loh, Phys. Rev. **175**, 533 (1968).

[17]M. J. Freiser, S. Methfessel, and F. Holtzberg, J. Appl. Phys. **39**, 900 (1968).

[18]K. E. Johnson and J. N. Sandoe, J. Chem. Soc. A 1964 (1969).

[19]A. Yanase and T. Kasuya, Prog. Theor. Phys. Suppl. **46**, 388 (1970).

[20]L. L. Chase, Phys. Rev. B **2**, 2308 (1970).

[21]H. A. Weakliem, C. H. Anderson, and E. S. Sabisky, Phys. Rev. B **2**, 4354 (1970).

[22]L. D. Merkle, R. C. Powell, and T. M. Wilson, J. Phys. C **11**, 3103 (1978).

[23]J. Hernandez A., W. K. Cory, and J. Rubio O., J. Chem. Phys. **72**, 198 (1980).

[24]T. Kobayasi, S. Mroczkowski, and J. Owen, J. Lunim. **21**, 247 (1980).

[25]J. Hernandez A., F. J. Lopez, H. Murrieta S., and J. Rubio O., J. Phys. Soc. Jpn. **50**, 225 (1981).

[26]R. Scheps, J. Electrochem. Soc. **136**, 1832 (1989).

[27]C. Pedrini, F. Rogemond, and D. S. McClure, J. Appl. Phys. **49**, 1196 (1986).

[28]A. de Cárcer, F. Cussó, and F. Jaque, Phys. Rev. B **38**, 10 812 (1988).

[29]R. L. Fuller and D. S. McClure, Phys. Rev. B **43**, 27 (1991).

[30]M. Godlewski, D. Hommel, J. M. Langer, and H. Przybylénska, J. Lumin. **24/25**, 217 (1981).

[31]B. Moine, C. Pedrini, and B. Courtois, J. Lumin. **50**, 31 (1991).

[32]S. A. Payne, L. L. Chase, H. W. Newkirk, L. K. Smith, and W. F. Krupke, IEEE J. Quantum Electron. **24**, 1077 (1988).

[33]D. J. Ehrlich, P. F. Moulton, and R. M. Osgood, Jr., Opt. Lett. **4**, 184 (1979).

[34]D. J. Ehrlich, P. F. Moulton, and R. M. Osgood, Jr., Opt. Lett. **5**, 339 (1980).

[35]K.-S. Lim and D. S. Hamilton, J. Opt. Soc. Am. **6**, 1401 (1989).

[36]W. J. Miniscalco, J. M. Pellegrino, and W. M. Yen, J. Appl. Phys. **49**, 6109 (1978).

[37]R. R. Jacobs, W. F. Krupke, and M. J. Weber, Appl. Phys. Lett. **33**, 410 (1978).

[38]G. J. Pogatshnik and D. S. Hamilton, Phys. Rev. B **36**, 8251 (1987).

[39]D. S. Hamilton, S. K. Gayen, G. J. Pogatshnik, and R. D. Chen, Phys. Rev. B **39**, 8807 (1989)